

Effect of thymoquinone on sepsis-induced cardiac damage *via* anti-inflammatory and anti-apoptotic mechanisms

Journal of International Medical Research

2022, Vol. 50(9) 1–13

© The Author(s) 2022

Article reuse guidelines:

sagepub.com/journals-permissions

DOI: 10.1177/03000605221118680

journals.sagepub.com/home/imr



Wenyan Guo¹, Xiaofeng Long¹, Mingyi Lv¹,
Shuling Deng¹, Duping Liu¹ and Qin Yang² 

Abstract

Objective: Sepsis is a systemic and deleterious host reaction to severe infection. Cardiac dysfunction is an established serious outcome of multiorgan failure associated with this condition. Therefore, it is important to develop drugs targeting sepsis-induced cardiac damage and inflammation. Thymoquinone (TQ) has anti-inflammatory, anti-oxidant, anti-fibrotic, anti-tumor, and anti-apoptotic effects. This study examined the effects of thymoquinone on sepsis-induced cardiac damage.

Methods: Male BALB/c mice were randomly segregated into four groups: control, TQ, cecal ligation and puncture (CLP), and CLP + TQ groups. CLP was performed after gavaging the mice with TQ for 2 weeks. After 48 hours, we estimated the histopathological changes in the cardiac tissue and the serum levels of cardiac troponin-T. We evaluated the expression of factors associated with inflammation, apoptosis, oxidative stress, and the PI3K/AKT pathway.

Results: TQ significantly reduced intestinal histological alterations and inhibited the upregulation of interleukin-6, tumor necrosis factor- α , Bax, NOX4, p-PI3K, and p-AKT. TQ also increased Bcl-2, HO-1, and NRF2 expression.

Conclusion: These results suggest that TQ effectively modulates pro-inflammatory, apoptotic, oxidative stress, and PI3K/AKT pathways, making it indispensable in the treatment of sepsis-induced cardiac damage.

¹Department of Intensive Care Units, Affiliated Zhongshan Hospital of Dalian University, No. 6 Jiefang Street, Dalian, China

²Department of Internal Medicine, The Affiliated Zhongshan Hospital of Dalian University, No. 6 Jiefang Street, Dalian, China

Corresponding author:

Xiaofeng Long, Department of Intensive Care Units, Affiliated Zhongshan Hospital of Dalian University. No. 6 Jiefang Street, Dalian 116001, China.
Email: longxiaofeng88@sina.com



Keywords

Sepsis, cardiac damage, thymoquinone, inflammation, apoptosis, oxidative stress, tumor necrosis factor

Date received: 23 March 2022; accepted: 18 July 2022

Introduction

Sepsis is a systemic, deleterious host reaction to severe infection, and it is recognized as one of the deadliest conditions in the intensive care unit.^{1,2} According to reports, the incidence of sepsis is 535 cases per 100,000 person-years, and it is continually rising. The in-hospital mortality rate is as high as 25% to 30%.³ Cardiac dysfunction is an established risk factor for multiorgan failure associated with this critical condition.⁴ Septic cardiac dysfunction has been associated with the excessive production of pro-inflammatory cytokines, including interleukin-6 (IL-6) and tumor necrosis factor- α (TNF- α), which also contribute to myocyte apoptosis and damage.⁵⁻⁷ In addition, previous studies demonstrated that the mechanisms underlying sepsis-induced myocardial dysfunction include inflammatory mediators, structural alterations, dysfunctional cardiomyocyte contractility, mitochondrial dysfunction, reduced energy metabolism, and cell death.⁸⁻¹³ Oxidative stress and inflammation are interdependent, and excessive reactive oxygen species (ROS) production at inflammatory sites can lead to oxidative stress, which in turn can induce mitochondrial damage.¹⁴ However, the precise mechanism of the pathogenesis of septic cardiomyopathy remains undefined.

In recent years, it has been reported that many active ingredients of natural drugs have viable anti-oxidant and anti-inflammatory effects and that they can exert protective effects against multiple cardiac diseases.¹⁴⁻¹⁶ A review concluded that

natural anti-oxidants can effectively protect myocardial and endothelial cells from stress-induced injury by regulating mitochondrial quality control.¹⁷ Chang *et al.* found that quercetin exerts cardioprotective effects by improving myocardial fibrosis and regulating mitophagy and endoplasmic reticulum stress.^{18,19} Thymoquinone (TQ, 2-isopropyl-5-methyl-1,4 benzoquinone), a natural phytochemical compound, is the main active component of *Nigella sativa* oil (commonly known as black cumin or black seed, an annual flowering plant native to Mediterranean countries).^{20,21} Several studies revealed that TQ has anti-inflammatory, anti-oxidant, anti-fibrotic, anti-tumor, and anti-apoptotic effects.²²⁻²⁵ Nagi *et al.* reported that TQ protected against doxorubicin-induced cardiac damage.²⁶

This study examined the utility of TQ for the treatment of sepsis-induced cardiac damage. Our results will contribute to clarification of the beneficial role and mechanism of action of TQ in sepsis-induced cardiac disorders.

Materials and methods

Animals

Male BALB/c mice were purchased from Beijing Vital River Lab Animal Technology Co., Ltd. (Beijing, China). All mice were housed in a room under controlled conditions (temperature, 23–25°C; humidity, 40%–60%; 12-hour/12-hour light/dark cycle).

Murine model of sepsis

To induce polymicrobial sepsis, an established murine model of cecal ligation and puncture (CLP) was used as previously described.²¹ The mice were anesthetized with sodium pentobarbital (100 mg/kg intraperitoneal injection). After surgically opening the peritoneum and exposing the bowel, two-thirds of the cecum were tied and cut with a 21-gauge needle. Gentle pressure was applied at the perforation sites to extrude a small amount of feces, which was then returned to the peritoneal cavity. Subsequently, the laparotomy site was stitched. The same procedure was applied in sham-operated mice, including surgical opening of the peritoneum and bowel exposure. However, needle perforation of the cecum and ligation were not performed. Eight-week-old male mice were randomly segregated into four groups (n = 12/group): control, TQ (100 mg/kg/day; Sigma-Aldrich, St. Louis, MO, USA), CLP, and CLP + TQ. CLP was performed after gavaging the mice with TQ for 2 weeks. After 48 hours, all surviving mice were killed, and blood samples were obtained from the inferior vena cava, collected in serum tubes, and stored at -80°C until further use. Coronal sections of the cardiac tissues were fixed in 10% formalin and then embedded in paraffin for histological evaluation. The remaining cardiac tissues were snap-frozen in liquid nitrogen for mRNA or immunoblotting analysis. All animal experiments were performed in accordance with the Guide for the Care and Use of Laboratory Animals. All animal experiments were approved by the Ethics Committee of Affiliated Zhongshan Hospital of Dalian University.

Serum analysis

Blood samples were collected, and the serum was stored at -80°C . The serum

concentrations of cardiac troponin-T (cTnT) were measured using an enzyme-linked immunosorbent assay kit (Westang, Shanghai, China).

Hematoxylin and eosin (H&E) staining

Cardiac tissues were fixed in 10% buffered formalin solution for 30 minutes and dehydrated in 75% ethanol overnight, followed by paraffin embedding. Serial sections ($4\ \mu\text{m}$, n = 3/group) were stained with H&E, and the lesion area in the cardiac tissue was observed using a BX40 upright light microscope (Olympus, Tokyo, Japan).

Masson's trichrome staining

Cardiac tissues were fixed in 10% buffered formalin solution for 30 minutes and dehydrated in 75% ethanol overnight, followed by paraffin embedding. Slides were stained with Masson's trichrome to investigate changes in cardiac tissues and observed using a BX40 upright light microscope. Blue staining indicated collagen accumulation.

RNA isolation and reverse transcription-quantitative PCR (RT-qPCR)

Total RNA was isolated from cardiac tissue and transcribed into complementary DNA (cDNA) using a TransScript One-Step gDNA Removal and cDNA Synthesis Supermix kit (Transgen, Beijing, China) according to the manufacturer's protocol. Gene expression was analyzed quantitatively by qPCR using a TransStart Top Green qPCR Supermix kit (Transgen). β -actin cDNA was amplified and quantitated in each cDNA preparation to normalize the relative amounts of the target genes. Primer sequences are listed in Table 1.

Immunohistochemistry (IHC)

Paraffin-embedded cardiac tissues were cut into $5\text{-}\mu\text{m}$ -thick cross-sections and

Table 1. Primer sequences.

Gene	Primers
TNF- α	Forward: 5'-TCTCATGCACCACCATCAAGGACT-3' Reverse: 5'-ACCACTCTCCCTTTGCAGAACTCA-3'
IL-6	Forward: 5'-TACCAGTTGCCTTCTTGGGACTGA-3' Reverse: 5'-TAAGCCTCCGACTTGTGAAGTGGT-3'
β -actin	Forward: 5'-CGATGCCCTGAGGGTCTTT-3' Reverse: 5'-GGATGCCACAGGATTCCAT-3'

TNF, tumor necrosis factor; IL, interleukin.

deparaffinized prior to staining using a standard protocol. Immunohistochemical staining was performed according to the manufacturer's instructions (Zsbio, Beijing, China) using antibodies against Bax (rabbit anti-Bax antibody, 1:200; Proteintech, Wuhan, China), Bcl-2 (rabbit anti-Bcl-2 antibody, 1:200; Proteintech), NRF2 (rabbit anti-NRF2 antibody, 1:200; Proteintech), NOX4 (rabbit anti-NOX4 antibody, 1:200; Proteintech), and HO-1 (rabbit anti-HO-1 antibody, 1:200; SOLARBIO, Beijing, China). All sections were examined using a BX40 upright light microscope.

TUNEL staining

The cardiac tissues were embedded in paraffin and serially sectioned to a thickness of 5 μ m. The sections were deparaffinized, hydrated in xylene and gradient concentrations of ethanol, incubated with proteinase K (37°C, 22 minutes), and stained using a Fluorescein TUNEL Cell Apoptosis Detection kit (Servicebio Technology Co., Ltd., Wuhan, China). All images were captured using a fluorescence microscope (Nikon). The cells that were positive for both TUNEL staining that aligned with DAPI staining were considered apoptotic cells and counted.

Western blot analysis

Proteins were extracted from cardiac tissues using radioimmunoprecipitation assay buffer (P0013B; Beyotime, Shanghai, China). First, the protein samples were separated using 10% sodium dodecyl sulfate-polyacrylamide gel electrophoresis and then transferred to polyvinylidene fluoride membranes (Immobilon, Millipore, Billerica, MA, USA). The membranes were blocked with 5% skimmed milk in TBST buffer (TBS containing 0.1% Tween-20) at room temperature for 1 hour and incubated with the primary antibodies at 4°C overnight. Primary antibodies against Bax (rabbit anti-Bax antibody, 1:1000; Proteintech, Wuhan, China), Bcl-2 (rabbit anti-Bcl-2 antibody, 1:1000, Proteintech, Wuhan, China), p-PI3K (rabbit anti-p-PI3K antibody, 1:500; BIOSS, Beijing, China), t-PI3K (rabbit anti-t-PI3K antibody, 1:2000, Proteintech), p-AKT (rabbit anti-p-AKT antibody, 1:2000, Proteintech), t-AKT (rabbit anti-t-AKT antibody, 1:2000, Proteintech), and β -actin (anti- β -actin, 1:1000; Cell Signaling Technology) were used. After three washes with TBS-T (15 minutes each), the membranes were incubated with the secondary antibody (anti-rabbit IgG, 1:1000; Cell Signaling Technology) for 1 hour. This analysis was performed independently three times.

The blotted proteins were quantified using ImageJ software (National Institutes of Health, Bethesda, MD, USA). β -actin was used as an internal control. Protein levels are expressed as protein/ β -actin ratios.

Statistical analysis

All data are presented as the mean \pm standard error of the mean. SPSS software v.23.0 (IBM, Armonk, NY, USA) was used to analyze all data. Differences among multiple groups were measured using one-way analysis of variance followed by Tukey's range test. $P < 0.05$ was considered statistically significant.

Results

Metabolic characterization

The metabolic characteristics of the mice in the four different groups are presented in Figure 1. The body/cardiac weight ratio did not differ among the four groups. At 48 hours after CLP injury, we observed a significant increase in serum cTnT levels in the CLP group compared with those in the control group ($P < 0.01$), but treatment with TQ significantly decreased serum cTnT levels ($P < 0.05$).

TQ reduced cardiac histopathological damage in the CLP group

H&E and Masson's trichrome were used to evaluate histopathological changes in cardiac tissues (Figure 2). Cardiac tissues appeared normal in control mice. CLP mice exhibited obvious pro-inflammatory cell infiltration compared with the findings in control and CLP + TQ mice. H&E staining revealed that TQ reduced leukocyte infiltration into the cardiac tissue of BALB/c mice. Collagen deposition was determined using Masson's staining. The CLP + TQ group displayed markedly reduced collagen deposition in cardiac tissue compared with the findings in the CLP group ($P < 0.05$). This result illustrated that TQ reduced fibrosis in cardiac tissue in BALB/c mice.

TQ inhibited apoptosis in cardiac tissues in the CLP group

To evaluate apoptosis in the cardiac tissues of mice in the four groups after treatment, TUNEL staining was performed. The number of TUNEL-positive cells was increased in the cardiac tissues of CLP mice compared with that in control mice ($P < 0.05$), whereas cardiac apoptosis was reduced in CLP + TQ mice ($P < 0.05$,

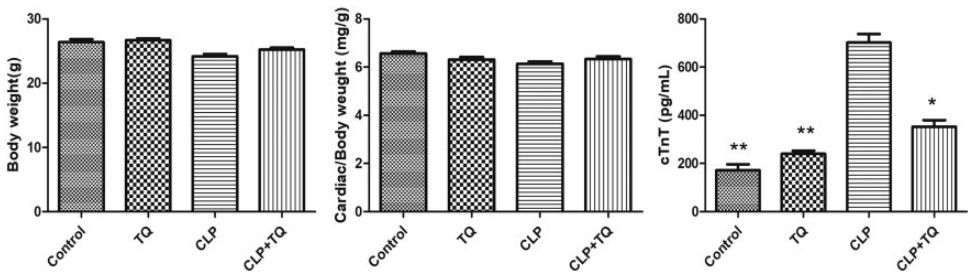


Figure 1. Cardiac/body weight ratio and serum cTnT levels in each group. Data are presented as the mean \pm standard error of the mean ($n = 7$ per group). * $P < 0.05$ vs. CLP group, ** $P < 0.01$ vs. CLP group. cTnT, cardiac troponin-T; CLP, cecal ligation and puncture; TQ, thymoquinone.

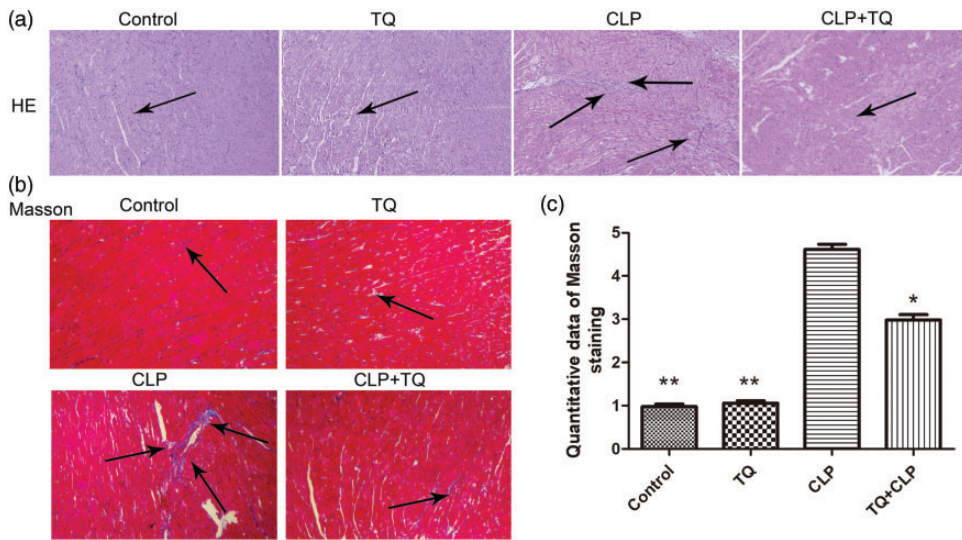


Figure 2. (a) Representative H&E staining of cardiac tissue from BALB/c mice in the four groups after treatment. The arrows indicate damage. Magnification, $\times 40$. (b) Representative images of Masson's trichrome staining of cardiac tissue from BALB/c mice in the four groups after treatment. The arrows indicate damage. Magnification, $\times 40$ and (c) Bar graph presenting the quantification of Masson's trichrome-positive cells. Data are presented as the mean \pm standard error of the mean ($n = 3$ per group). * $P < 0.05$ vs. CLP group, ** $P < 0.05$ vs. CLP group. CLP, cecal ligation and puncture; TQ, thymoquinone.

Figure 3a and c). Bax and Bcl-2 gene and protein expression was measured using immunohistochemistry and western blotting, respectively (Figure 3). Bax expression was higher in the CLP group than in the control group ($P < 0.05$). This increase was attenuated in the CLP+TQ group ($P < 0.05$). Interestingly, the expression of Bcl-2 displayed the opposite trend. Compared with its control expression, Bcl-2 expression was decreased in the CLP group ($P < 0.05$), and this decrease was attenuated by TQ treatment ($P < 0.05$). This result demonstrated that TQ inhibited apoptosis in CLP mice by suppressing the upregulation of Bax and downregulation of Bcl-2.

TQ inhibited pro-inflammatory cytokine expression in the cardiac tissue of CLP mice

IL-6 and TNF- α gene expression was measured by real-time PCR (Figure 4) to evaluate

the involvement of pro-inflammatory cytokines in the cardiac tissue changes in the four groups. IL-6 and TNF- α gene expression was higher in the CLP group than in the control group (both $P < 0.05$). However, this increase was attenuated in the TQ+CLP group (both $P < 0.05$).

TQ inhibited oxidative stress in the cardiac tissue of CLP group

To evaluate oxidative stress in cardiac tissues in the four groups after treatment, IHC of HO-1, NRF2, and NOX4 was performed (Figure 5). We observed an increase in NOX4 expression and decreases in HO-1 and NRF2 expression in the CLP group compared with the findings in the control group (all $P < 0.05$). However, TQ treatment inhibited the upregulation of NOX4 and downregulation of HO-1 and NRF2 (all $P < 0.05$).

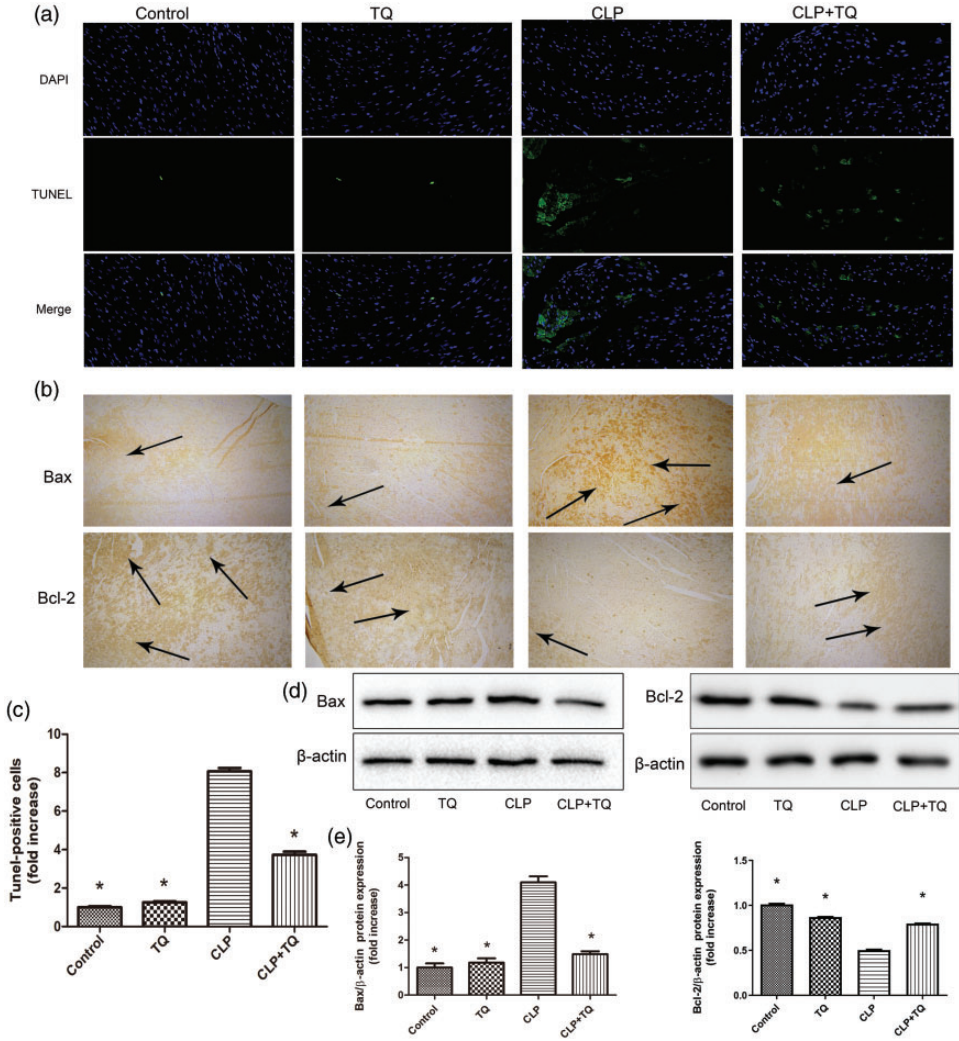


Figure 3. (a) TUNEL- (green fluorescence) and DAPI-stained (blue fluorescence) photomicrographs. Magnification, $\times 40$. (c) Quantification of apoptotic cardiomyocytes. $*P < 0.05$ vs. CLP group. (b) Representative immunohistochemical staining for Bax and Bcl-2 in cardiac tissue. Magnification, $\times 40$. Arrows indicate positively stained cells ($n = 3$). (d) Immunoblotting for Bax and Bcl-2 in cardiac tissue and (e) Bar graph presenting the quantification of Bax and Bcl-2 protein expression. Data are presented as the \pm standard error of the mean ($n = 3$ per group). $*P < 0.05$ vs. CLP group. CLP, cecal ligation and puncture; TQ, thymoquinone.

TQ inhibits PI3K/AKT pathways in cardiac tissue of CLP group mice

To investigate the effect of TQ on regulation of the PI3K/AKT signaling pathway, immunoblotting with PI3K and AKT were

performed (Figure 6). We observed increases in p-PI3K and p-AKT expression in CLP mice compared with that in control mice (both $P < 0.05$); however, these increases were markedly suppressed in the TQ + CLP group (both $P < 0.05$).

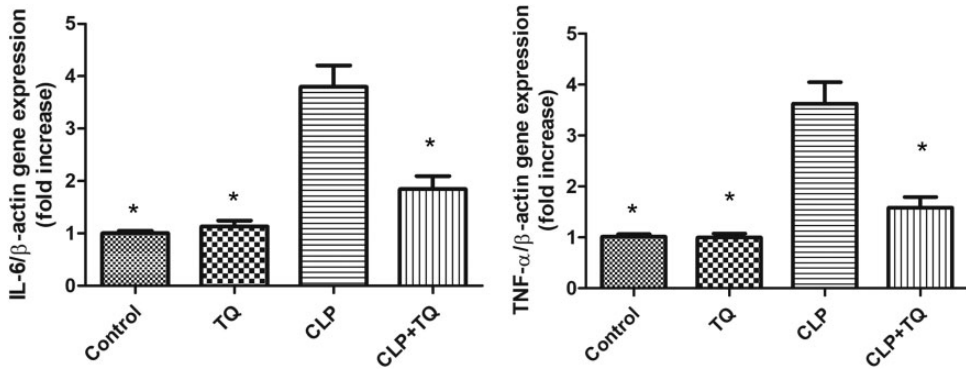


Figure 4. Relative mRNA expression of IL-6 and TNF- α expression in cardiac tissue from mice in the four groups after treatment. Data are presented as the mean \pm standard error of the mean ($n=3$ per group). * $P < 0.05$ vs. CLP group.

IL, interleukin; TNF, tumor necrosis factor; CLP, cecal ligation and puncture; TQ, thymoquinone.

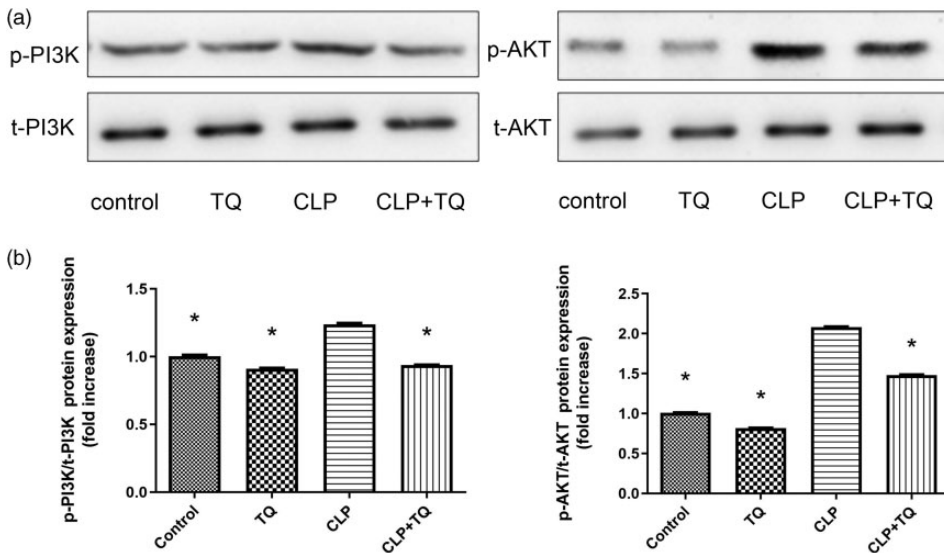


Figure 5. (a) Representative immunohistochemical staining for NOX4, NRF2, and HO-1. Magnification, $\times 40$. Arrows indicate positively stained cells ($n=3$). (b) Bar graph presenting the quantification of NOX4-, NRF2-, and HO-1-stained cells. Data are presented as the mean \pm standard error of the mean ($n=3$ per group). * $P < 0.05$ vs. CLP group.

CLP, cecal ligation and puncture; TQ, thymoquinone.

Discussion

This study demonstrated that TQ exerts protective effects against sepsis-induced cardiac damage through anti-inflammatory, anti-apoptosis, and anti-oxidant effects and

the inhibition of PI3K phosphorylation (Figure 7).

We established a sepsis-induced cardiac damage model *via* CLP surgery to investigate the effects of TQ. Regarding metabolic

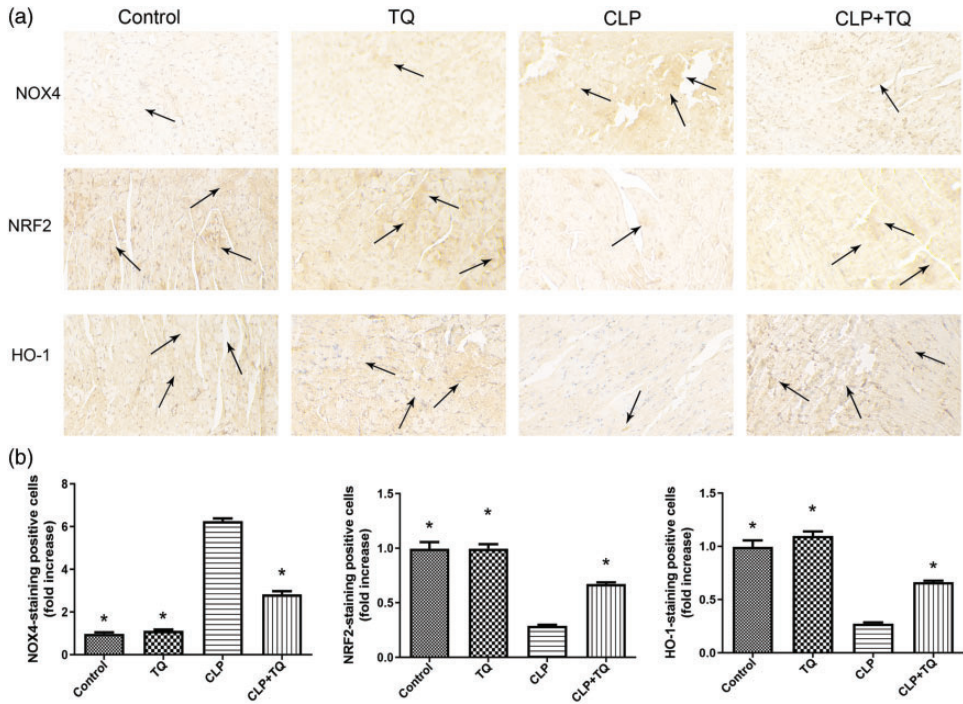


Figure 6. (a) Immunoblotting for p-PI3K and p-AKT in cardiac tissue and (b) Bar graph presenting the quantification of p-PI3K and p-AKT protein expression. Data are presented as the mean \pm standard error of the mean ($n = 3$ per group). * $P < 0.05$ vs. CLP group. CLP, cecal ligation and puncture; TQ, thymoquinone.

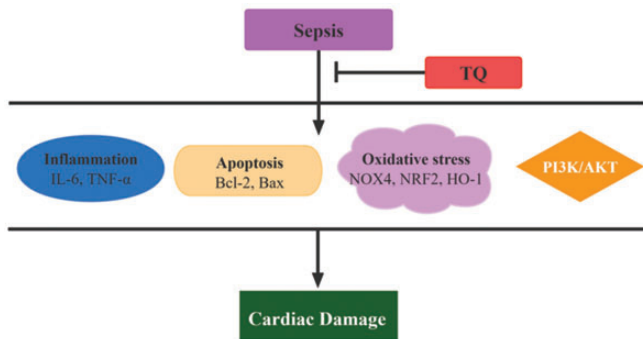


Figure 7. Diagram of the mechanism by which TQ suppresses sepsis-induced cardiac damage. IL, interleukin; TNF, tumor necrosis factor; TQ, thymoquinone.

characteristics, cTnT has high specificity, and its levels are directly proportional to the degree of myocardial damage.²⁸ In our study, the CLP group displayed

significantly higher cTnT levels than the control group. However, treatment with TQ markedly reduced serum cTnT levels, thereby alleviating sepsis-induced cardiac

damage. These results are in agreement with a report by Chu *et al.*²⁹ In addition, H&E and Masson's trichrome staining revealed obvious pro-inflammatory cell infiltration and collagen deposition in the CLP group; however, these histopathological changes were suppressed in the CLP + TQ group. Thus, TQ reduced histopathological changes in cardiac tissue in BALB/c mice.

Apoptosis, a form of programmed cell death, plays a critical role in sepsis-induced multiorgan dysfunction syndrome.³⁰ A previous study reported that inhibition of myocardial apoptosis is related to the improvement of cardiac function in mice with sepsis.^{31,32} The key regulators of apoptosis are members of the Bcl-2 family of proteins. This protein family features a variety of pro-apoptotic (e.g., Bax, Bak) and anti-apoptotic (e.g., Bcl-2, Bcl-xL, Bcl-w) proteins.^{33,34} In the current study, Bax protein expression was increased and Bcl-2 protein expression was decreased in the CLP group compared with that in the control group. It is worth noting that TQ inhibited the expression of Bax and enhanced that of Bcl-2, suggesting that apoptosis was inhibited.

Inflammation is an important mechanism of myocardial injury in sepsis that can mediate apoptosis and oxidative stress. During sepsis, it is believed that increased systemic levels of endotoxins activate immune cells, which in turn promote the production of inflammatory mediators and cytokines.³⁵ Pro-inflammatory genes (e.g., TNF- α , IL-6) are reportedly expressed at high levels in sepsis, and they are responsible for cardiac damage.^{36,37} As mentioned previously, we observed increased apoptosis *in vivo*, and IL-6 and TNF- α expression was obviously higher in the CLP group than in the control group. This increase was significantly inhibited by treatment with TQ. This illustrated that TQ acts against sepsis-induced pro-inflammatory cytokine release.

Oxidative stress and inflammation are interdependent. Oxidative stress is considered an important factor in the pathogenesis of cardiovascular disease.³⁸ NOX-derived ROS promote coronary microvascular damage, which then causes aberrant apoptosis, inflammation, and fibrosis.³⁹ It has been reported that natural anti-oxidants protect myocardial and endothelial cells against oxidative stress.^{17,40} In this study, we examined the expression of anti-oxidant oxidative stress indicators. We detected decreases of HO-1 and NRF2 expression and an increase of NOX4 expression in the CLP group, but TQ treatment inhibited these changes. Xing *et al.* reported that a natural antioxidant (puerarin) can regulate inflammatory responses and oxidative stress injury induced by LPS.¹⁴

Autophagy is a type II cell death mechanism. Mitochondrial autophagy induced by LPS-induced sepsis contributes to cardiac dysfunction.⁴¹ Akt phosphorylation has been found to prevent apoptosis and promote cell survival in the ischemic heart.⁴² In numerous studies on sepsis, PI3K and its downstream target AKT have been reported to participate in the regulation of cell activation, inflammation, and apoptosis.^{43,44} Chen *et al.* observed that inhibition of the PI3K/AKT signaling pathway can mitigate sepsis-induced myocardial injury.⁴⁵ The present study evaluated the effect of TQ on PI3K and demonstrated that PI3K expression was markedly higher in the CLP group than in the control group. Interestingly, TQ treatment reversed the increase in PI3K expression, demonstrating that TQ acted against sepsis induced-cardiac damage by inhibiting PI3K signaling.

In fact, mitochondrial dysfunction, as typified by inflammation, oxidative stress, and apoptosis, is a fundamental challenge in cardiomyopathy.^{16,46,47} This study had several limitations. First, we did not directly detect mitochondrial damage. In future experiments, we will conduct in-depth

experiments and further detect mitochondrial damage. In addition, we only performed *in vivo* studies. We will conduct cell experiments to verify the specific mechanisms and pathways in the future.

Conclusion

Our study established that TQ has a protective effect on sepsis-induced cardiac damage as demonstrated by the downregulation of cTnT and suppression of inflammatory cell infiltration, pro-inflammatory cytokine expression, apoptosis, oxidative stress, and PI3K/AKT pathway activation. These findings provide novel insight into cardiac damage caused by sepsis and present the possibility of a new therapeutic intervention for the treatment of cardiovascular diseases.

Author contributions

Wenyan Guo designed this study. Mingyi Lv and Qin Yang helped perform experiments. Wenyan Guo and Shuling Deng analyzed data and interpreted the results of the experiments. Duping Liu prepared figures. Qin Yang drafted the manuscript. Wenyan Guo helped revise the manuscript. Xiaofeng Long provided the research funds. All authors read and approved the final manuscript.

Data availability statement

All data can be obtained from the corresponding author.


Declaration of conflicting interest

The authors declare that they have no conflicts of interest.

Funding

The study was supported by a grant from the Dalian Medical Science Research Program of China (grant no. 1911109).

ORCID iD

Qin Yang  <https://orcid.org/0000-0003-3566-8898>

References

1. Shankar-Hari M, Phillips GS, Levy ML, et al. Developing a New Definition and Assessing New Clinical Criteria for Septic Shock: For the Third International Consensus Definitions for Sepsis and Septic Shock (Sepsis-3). *Jama* 2016; 315: 775–787.
2. Angus DC, Linde-Zwirble WT, Lidicker J, et al. Epidemiology of severe sepsis in the United States: analysis of incidence, outcome, and associated costs of care. *Crit Care Med* 2001; 29: 1303–1310.
3. Fleischmann C, Scherag A, Adhikari NK, et al. Assessment of Global Incidence and Mortality of Hospital-treated Sepsis. Current Estimates and Limitations. *Am J Respir Crit Care Med* 2016; 193: 259–272.
4. Zanotti-Cavazzoni SL and Hollenberg SM. Cardiac dysfunction in severe sepsis and septic shock. *Curr Opin Crit Care* 2009; 15: 392–397.
5. Sharma AC, Motew SJ, Farias S, et al. Sepsis alters myocardial and plasma concentrations of endothelin and nitric oxide in rats. *J Mol Cell Cardiol* 1997; 29: 1469–1477.
6. Damas P, Ledoux D, Nys M, et al. Cytokine serum level during severe sepsis in human IL-6 as a marker of severity. *Ann Surg* 1992; 215: 356–362.
7. Buerke U, Carter JM, Schlitt A, et al. Apoptosis contributes to septic cardiomyopathy and is improved by simvastatin therapy. *Shock (Augusta, Ga)* 2008; 29: 497–503.
8. Merx MW and Weber C. Sepsis and the heart. *Circulation* 2007; 116: 793–802.
9. Rudiger A and Singer M. Mechanisms of sepsis-induced cardiac dysfunction. *Crit Care Med* 2007; 35: 1599–1608.
10. Bayeva M, Sawicki KT, Butler J, et al. Molecular and cellular basis of viable dysfunctional myocardium. *Circ Heart Fail* 2014; 7: 680–691.
11. Association CDBoCMD. Chinese expert consensus on smoking cessation intervention for cardiovascular diseases. *Chin J Intern Med* 2012; 51: 168–173.
12. Zhu H, Toan S, Mui D, et al. Mitochondrial quality surveillance as a therapeutic target in myocardial infarction. *Acta Physiol (Oxf)* 2021; 231: e13590.

13. Wang J and Zhou H. Mitochondrial quality control mechanisms as molecular targets in cardiac ischemia-reperfusion injury. *Acta Pharm Sin B* 2020; 10: 1866–1879.
14. Chang X, Zhang T, Liu D, et al. Puerarin Attenuates LPS-Induced Inflammatory Responses and Oxidative Stress Injury in Human Umbilical Vein Endothelial Cells through Mitochondrial Quality Control. *Oxid Med Cell Longev* 2021; 2021: 6659240.
15. Chang X, Yao S, Wu Q, et al. Tongyang Huoxue Decoction (TYHX) Ameliorating Hypoxia/Reoxygenation-Induced Disequilibrium of Calcium Homeostasis and Redox Imbalance via Regulating Mitochondrial Quality Control in Sinoatrial Node Cells. *Oxid Med Cell Longev* 2021; 2021: 3154501.
16. Wang J, Chen P, Cao Q, et al. Traditional Chinese Medicine Ginseng Dingzhi Decoction Ameliorates Myocardial Fibrosis and High Glucose-Induced Cardiomyocyte Injury by Regulating Intestinal Flora and Mitochondrial Dysfunction. *Oxid Med Cell Longev* 2022; 2022: 9205908.
17. Chang X, Zhao Z, Zhang W, et al. Natural Antioxidants Improve the Vulnerability of Cardiomyocytes and Vascular Endothelial Cells under Stress Conditions: A Focus on Mitochondrial Quality Control. *Oxid Med Cell Longev* 2021; 2021: 6620677.
18. Chang X, Zhang T, Wang J, et al. SIRT5-Related Desuccinylation Modification Contributes to Quercetin-Induced Protection against Heart Failure and High-Glucose-Prompted Cardiomyocytes Injured through Regulation of Mitochondrial Quality Surveillance. *Oxid Med Cell Longev* 2021; 2021: 5876841.
19. Chang X, Zhang T, Meng Q, et al. Quercetin Improves Cardiomyocyte Vulnerability to Hypoxia by Regulating SIRT1/TMBIM6-Related Mitophagy and Endoplasmic Reticulum Stress. *Oxid Med Cell Longev* 2021; 2021: 5529913.
20. Woo CC, Kumar AP, Sethi G, et al. Thymoquinone: potential cure for inflammatory disorders and cancer. *Biochem Pharmacol* 2012; 83: 443–451.
21. Ahmad N, Ahmad R, Alam MA, et al. Quantification and evaluation of thymoquinone loaded mucoadhesive nanoemulsion for treatment of cerebral ischemia. *Int J Biol Macromol* 2016; 88: 320–332.
22. Gali-Muhtasib H, Roessner A and Schneider-Stock R. Thymoquinone: a promising anti-cancer drug from natural sources. *Int J Biochem Cell Biol* 2006; 38: 1249–1253.
23. Sheikhabaei F, Khazaei M, Rabzia A, et al. Protective Effects of Thymoquinone against Methotrexate-Induced Germ Cell Apoptosis in Male Mice. *Int J Fertil Steril* 2016; 9: 541–547.
24. Amin B and Hosseinzadeh H. Black Cumin (*Nigella sativa*) and Its Active Constituent, Thymoquinone: An Overview on the Analgesic and Anti-inflammatory Effects. *Planta Med* 2016; 82: 8–16.
25. Bai T, Lian LH, Wu YL, et al. Thymoquinone attenuates liver fibrosis via PI3K and TLR4 signaling pathways in activated hepatic stellate cells. *Int Immunopharmacol* 2013; 15: 275–281.
26. Nagi MN and Mansour MA. Protective effect of thymoquinone against doxorubicin-induced cardiotoxicity in rats: a possible mechanism of protection. *Pharmacol Res* 2000; 41: 283–289.
27. Rittirsch D, Huber-Lang MS, Flierl MA, et al. Immunodesign of experimental sepsis by cecal ligation and puncture. *Nat Protoc* 2009; 4: 31–36.
28. Mair J. Cardiac troponin I and troponin T: are enzymes still relevant as cardiac markers? *Clin Chim Acta* 1997; 257: 99–115.
29. Chu M, Gao Y, Zhang Y, et al. The role of speckle tracking echocardiography in assessment of lipopolysaccharide-induced myocardial dysfunction in mice. *J Thorac Dis* 2015; 7: 2253–2261.
30. Oberholzer C, Oberholzer A, Clare-Salzler M, et al. Apoptosis in sepsis: a new target for therapeutic exploration. *FASEB J* 2001; 15: 879–892.
31. Gao M, Ha T, Zhang X, et al. Toll-like receptor 3 plays a central role in cardiac dysfunction during polymicrobial sepsis. *Crit Care Med* 2012; 40: 2390–2399.
32. Ha T, Hua F, Grant D, et al. Glucan phosphate attenuates cardiac dysfunction and inhibits cardiac MIF expression and apoptosis in septic mice. *Am J Physiol Heart Circ Physiol* 2006; 291: H1910–H1918.

33. Youle RJ and Strasser A. The BCL-2 protein family: opposing activities that mediate cell death. *Nat Rev Mol Cell Biol* 2008; 9: 47–59.
34. Chipuk JE, Moldoveanu T, Llambi F, et al. The BCL-2 family reunion. *Mol Cell* 2010; 37: 299–310.
35. Jekarl DW, Kim KS, Lee S, et al. Cytokine and molecular networks in sepsis cases: a network biology approach. *Eur Cytokine Netw* 2018; 29: 103–111.
36. Kakihana Y, Ito T, Nakahara M, et al. Sepsis-induced myocardial dysfunction: pathophysiology and management. *J Intensive Care* 2016; 4: 22.
37. Pfeiffer D, Roßmanith E, Lang I, et al. miR-146a, miR-146b, and miR-155 increase expression of IL-6 and IL-8 and support HSP10 in an In vitro sepsis model. *PLoS one* 2017; 12: e0179850.
38. Chang X, Zhang T, Zhang W, et al. Natural Drugs as a Treatment Strategy for Cardiovascular Disease through the Regulation of Oxidative Stress. *Oxid Med Cell Longev* 2020; 2020: 5430407.
39. Chang X, Lochner A, Wang HH, et al. Coronary microvascular injury in myocardial infarction: perception and knowledge for mitochondrial quality control. *Theranostics* 2021; 11: 6766–6785.
40. Chang X, Zhang W, Zhao Z, et al. Regulation of Mitochondrial Quality Control by Natural Drugs in the Treatment of Cardiovascular Diseases: Potential and Advantages. *Front Cell Dev Biol* 2020; 8: 616139.
41. Wang Y, Jasper H, Toan S, et al. Mitophagy coordinates the mitochondrial unfolded protein response to attenuate inflammation-mediated myocardial injury. *Redox Biol* 2021; 45: 102049.
42. Li H, Song F, Duan LR, et al. Paeonol and danshensu combination attenuates apoptosis in myocardial infarcted rats by inhibiting oxidative stress: Roles of Nrf2/HO-1 and PI3K/Akt pathway. *Sci Rep* 2016; 6: 23693.
43. An R, Zhao L, Xi C, et al. Melatonin attenuates sepsis-induced cardiac dysfunction via a PI3K/Akt-dependent mechanism. *Basic Res Cardiol* 2016; 111: 8.
44. Kim TH, Kim SJ and Lee SM. Stimulation of the $\alpha 7$ nicotinic acetylcholine receptor protects against sepsis by inhibiting Toll-like receptor via phosphoinositide 3-kinase activation. *J Infect Dis* 2014; 209: 1668–1677.
45. Chen L, Liu P, Feng X, et al. Salidroside suppressing LPS-induced myocardial injury by inhibiting ROS-mediated PI3K/Akt/mTOR pathway in vitro and in vivo. *J Cell Mol Med* 2017; 21: 3178–3189.
46. Sun D, Wang J, Toan S, et al. Molecular mechanisms of coronary microvascular endothelial dysfunction in diabetes mellitus: focus on mitochondrial quality surveillance. *Angiogenesis* 2022; 25: 307–329.
47. Wang S, Zhu H, Li R, et al. DNA-PKcs interacts with and phosphorylates Fis1 to induce mitochondrial fragmentation in tubular cells during acute kidney injury. *Sci Signal* 2022; 15: eabh1121.